Since January 2020 Elsevier has created a COVID-19 resource centre with free information in English and Mandarin on the novel coronavirus COVID-19. The COVID-19 resource centre is hosted on Elsevier Connect, the company's public news and information website.

Journal of the Taiwan Institute of Chemical Engineers 42 (2011) 5–12

Contents lists available at ScienceDirect

Journal of the Taiwan Institute of Chemical Engineers

journal homepage: www.elsevier.com/locate/jtice

Effect of co-axially hybridized gene targets on hybridization efficiency of microarrayed DNA probes

Kai Ren Jiang [a], Jie-Len Huang [b], Chia-Chun Chen [b], Hung-Ju Su [b,*], Jui-Chuang Wu [a,*]

[a] Chemical Engineering Department, Chung Yuan Christian University, Chung Li, Tao Yuan 32023, Taiwan
[b] Biomedical Engineering Center, Industrial Technology Research Institute, Chu Tung, Hsin Chu 31040, Taiwan

ARTICLE INFO

Article history:
Received 14 December 2009
Received in revised form 19 April 2010
Accepted 25 April 2010

Keywords:
Hybridization efficiency
DNA microarray
Molecular steric hindrance
DNA biochips
DNA pre-hybridization

ABSTRACT

The effect of relative size of two co-axially hybridized gene targets on the hybridization efficiency was studied for two DNA probe configurations and various probe concentrations. Each of two sets of microarrayed probes contained a pair of DNA probes and a pair of their complementary samples labeled with two distinct fluorescent dyes. The sequence of each probe is especially designed so that two targets are simultaneously complementary to two adjacent sections of the probe. The molecular steric effect on the hybridization efficiency is investigated by comparing the dye signals between configurations of one-target and two-target hybridization scenarios. The results show that a low probe concentration gives better hybridization efficiency and the first-hybridization conducted by a shorter-size DNA target improves the hybridization efficiency of the second target coupling onto the same probe.

1. Introduction

Since the completion of human gene decoding project in the 1990s, microarray analyses have been widely applied on gene expression (Kan *et al.*, 2006; Ruuska *et al.*, 2002), diagnosis of influenza viruses (Dawson *et al.*, 2006), and many other fields (Wang and Cheng, 2005). Microarrays are promising alternatives which surpass the potential of sequencing since they can detect thousands of genes in parallel. Further development of this technology is still underway, particularly in the area of improving the hybridization efficiency of immobilized DNA probes with their sample targets. The current research efforts are rooted on the understanding that the hybridization efficiency directly indicates the success of the experimental design and further data interpretation.

There were several current methodologies to measure the DNA hybridization efficiency. The combination measurement of height and elastic compressibility of ss-DNA was verified an effective approach to detect the hybridization of nanostructured DNA (Mirmomtaz *et al.*, 2008). The surface plasmon resonance (SPR) spectroscopy is an in situ label-free optical method to dynamically detect the hybridization efficiency in the measurement of total-refraction angles (Peterson *et al.*, 2001). The X-ray photoelectron spectroscopy (XPS) is another potential tool to measure DNA hybridization efficiency by its detection on the phosphorus elemental composition, which specifically exists in a DNA strand (Liu *et al.*, 2009). The gold nanoparticles provide an advantage of rapid visual detection on DNA hybridization, but its applications are confined due to the lack of signal dynamic ranges (Mao *et al.*, 2009). The fluorescence labeling is still the traditional and popular methodology due to its convenient interpretation and excellent dynamic range of signal intensity, which is supposed to measure in proportion by one-fluorescent dye corresponding to one DNA molecule (McQuain *et al.*, 2004; Peytavi *et al.*, 2005).

The hybridization efficiency of DNA chips is critically affected by the overall conditions, for instance, probe immobilization (Zammatteo *et al.*, 2000), probe density (Peterson *et al.*, 2001), addition of a stabilizer (Maruyama *et al.*, 2001), and hybridization conditions such as incubation temperature and salt concentration (Rule *et al.*, 1997), electric field (Fixe *et al.*, 2004), agitation or mixing (Deng *et al.*, 2006; McQuain *et al.*, 2004), and substrate surface conditions (Guo *et al.*, 1994; Wu *et al.*, 2006). In addition to these overall conditions, the molecular-level studies has also been reported to improve the hybridization efficiency of microarrayed DNA, such as immobilization of double-stranded probes (Razumovitch *et al.*, 2009), nucleotide structure of probe and target (Koehler and Peyret, 2005), probe size and mismatch position (Letowski *et al.*, 2004), effect of blocking oligo (Tao *et al.*, 2003), effect of overhang size on probes (Peytavi *et al.*, 2005), DNA secondary structure (Koehler and Peyret, 2005), and target pre-hybridization (Yang *et al.*, 2008). However, these research efforts

* Corresponding authors.
E-mail addresses: suhungju@itri.org.tw (H.-J. Su), ray_j_wu@cycu.edu.tw (J.-C. Wu).

1876-1070/$ – see front matter © 2010 Taiwan Institute of Chemical Engineers. Published by Elsevier B.V. All rights reserved.
doi:10.1016/j.jtice.2010.04.012

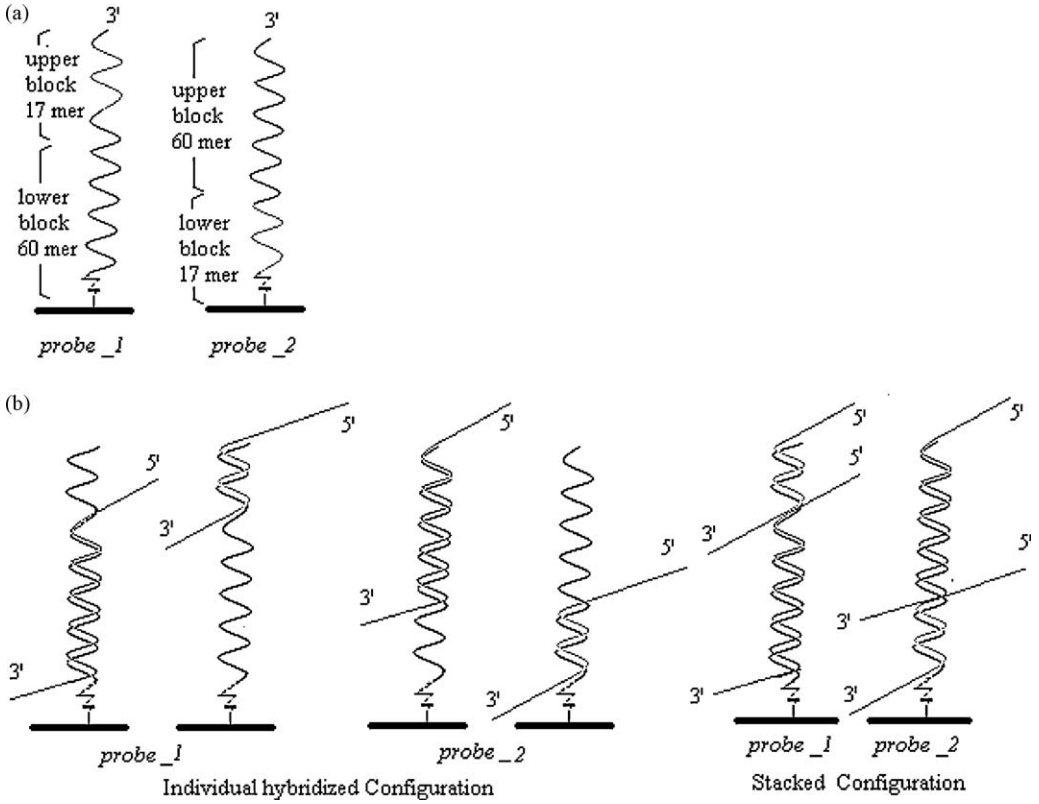

Fig. 1. Experimental design of the DNA probes with their complementary targets. (a) Two types of oligo nucleotide probes composed of two identical but reverse-sequence blocks. Probe_1 has a 17-mer block stacked adjacent at the top and 60-mer block at the bottom. Probe_2 has the identical sequence of blocks but the location is inverted. (b) The individual-hybridized and stacked configurations.

have mostly been confined to non-gene targets. The manipulation and detection of a signature gene target actually is its corresponding gene product, particularly which states more directly toward the realistic applications of diagnosis.

In this study, we conducted a very direct investigation on a realistic system of gene targets. Their probes were immobilized on planar slides with two reverse sequential blocks. We designed three sets of targets, with each set having one plant and one human gene. These two quite distinct species were selected to ensure the minimum opportunity for cross-hybridization between each other. Each set of targets hybridized onto the sequential blocks of their shared probes in a coaxial stacking configuration, *i.e.* hybridizing immediately next to each other along the continuous complement probe strand, as shown in Fig. 1. The relatively reverse sequential blocks on two probes indicate the steric effect of hybridization position. Another parameter investigated was the relative size of pre-hybridization target to its up-coming stacking neighbor. Three pairs of plant/human gene targets were selected to address this issue in relative sizes of 528mer/1027mer, 690mer/313mer, and 1020mer/432mer. The hybridization efficiency was investigated by comparing the individual hybridization schemes with the stacking ones based on the detection signals of the labeling dyes. This provides further understanding for what conditions of the pre-hybridization of a gene target enhance the hybridization efficiency of next target coupling onto the same probe.

2. Experimental

2.1. Materials

Arabidopsis thaliana plasmid was adopted as the first species source of DNA target. It was the first plant genome to be sequenced and now becomes popular as a model organism in plant biology and genetics (Lorkovic, 2009; Sandoval *et al.*, 2008). Three genetic sections of this plant were cloned and notated as pda13015 (528b), pda06175 (690b), and pda06122 (1020b). Their final PCR products were labeled with Cy5 fluorescent dye to serve as the genetic targets. The second species is human gene in total RNA, and its PCR products include ATP5O (313b), PSMA5 (432b), and CANX (1027b) and labeled with Cy3 dye as targets. ATP5O was known functioned as a human ATP synthase and CANX a homo sapiens calnexin. ATP5O is the most significantly reduced gene involved in the oxidative phosphorylation (OXPHOS) (Mootha *et al.*, 2003), which was reported in parallel with increased insulin resistance in patients with type II diabetes mellitus (Sreekumar *et al.*, 2002) CANX is a molecular chaperone found primarily in the endoplasmic reticulum and is essential for proper protein folding. Correct protein assembly in the membrane is supported by CANX, which retains intermediate structures in the endoplasmic reticulum prior to ternary complex formation completion (Takizawa *et al.*, 2004). As for the human PSMA5, very little is known about its function and self-aggregation up to now. A recent report indicated that it exists mainly as tetramer (Han *et al.*, 2004). The corresponding information of all genetic targets can be found from Table 1.

We also used T7-17-Cy3 (17mer) as the negative-control target to check the non-specific hybridization. T7-17 is a complete sequence of plant expression vector pDuExB2 (NCBI Database EF565885.1) with sequence 5′-ATACGACTCACTATAGG-3′-Cy3. SP5-Cy5 (60mer) serves as an immobilization control probe with sequence 5′-GCTGTAACTTATCACACCGTTTCTACAGGTTAGCTAAC-GAGTGTGCGCAAGTATTAAGTG-amine-3′-C6-Cy5, which is a complete genome of SARS coronavirus strain CV7 (NCBI Database DQ898174.1)

DNA probes are with 5′-end amino linker modification to covalently attach themselves onto the chemically coated glass

Table 1
Information of genetic DNA targets adopted in this study. *Arabidopsis thaliana* and human served as the species sources.

Genetic target	Length (bases)	Definition (NCBI gene bank)
pda06175	690	*Arabidopsis thaliana* unknown protein (At1g62250) mRNA, complete cds.
pda06122	1020	*Arabidopsis thaliana* putative NAM protein (At1g52890) mRNA, complete cds.
pda13015	528	*Arabidopsis thaliana* clone RAFL15-32-O04 (R20961) putative protein kinase (At1g76370) mRNA, partial cds.
ATP5O	313	ATP synthase, H+ transporting, mitochondrial F1 complex, O subunit (oligomycin sensitivity conferring protein).
PSMA5	432	PSMA5: proteasome (prosome, macropain) subunit, alpha type, 5.
CANX	1027	Homo sapiens calnexin (CANX), transcript variant 1, mRNA.

slides (Phalanx Biotech, Hsinchu, Taiwan). Two sets of probes are denoted as *a*, *b*, and *c*, and each set includes two types of sequence orientation, _1 and _2. These two types possess two identical but constituent blocks. For instance, probes *a*_1 and *a*_2, they are composed with *pda06175c* (17mers) and *ATP5Oc* (60mers), but the orders of these two blocks are reverse. Table 1 also shows the complementary section of each target with its coupling probe. All DNA target, probes, and PCR primers are purchased or synthesized from ScinoPharm (Tainan, Taiwan) and concentrations were quantified by excluding modified and fluorescent molecules. The chemically coated DNA chips were provided by Phalanx Biotech (Hsinchu, Taiwan). The RT-PCR kit to reversely transcript human RNA to cDNA was purchased from Invitrogen (SuperScript™ II RT). The buffer for preparing probe microarrays is a mixture of 20× SSC (Amresco), glycerol (100%, ICN Biomedicals), and ddH_2O (Milli-Q synthesis A10 system). The wash step used a series of concentrations of sodium dodecyl sulfate (SDS) and SSC buffers, both purchased from Amresco.

2.2. Instruments

Microarrays were printed with a Cartesian none-contact microarrayer (PixSys7500, Genomic Solutions, Michigan, USA). Before the hybridization step, targets were pre-heated to 95 °C on a GeneAmp_PCR machine (9700, Applied Biosystems, California, USA). Hybridization results were scanned on a GenePix Microarray scanner (4000B, Molecular Devices, California, USA). The hybridization was incubated in a Cocoon hybridization incubator (Bersing Bioscience Tech, Hsinchu, Taiwan) equipped with a plate shaking function. The DNA-chip washing was performed on a Firstek orbital shaker (S101D, Firstek Scientific, Taipei, Taiwan). The TaKaRa™ spaced cover glass for hybridization was purchased from TaKaRa Biotechnology (Shiga, Japan). Wet chips were spun off to dry by a mini spinner (BTCPC100, Bersing Bioscience Tech, Hsinchu, Taiwan).

3. Experimental procedure

3.1. Preparation of plant ssDNA targets

In order to carry out the asymmetric Polymerase Chain Reaction (PCR), 2 μl of 50 ng/μl *Arabidopsis thaliana* plasmid was mixed with 50 μl PCR mixture, which contains 10 mM dNTP, 5 U/μl Taq DNA polymerase, 10× PCR buffer, 2 μl of 10 μM reverse primer, 2 μl of 0.2 μM forward primer, and ddH_2O. As shown in Table 2, three reverse primers separately added in three tubes are cy5-pda06175-R, cy5-pda06122-R, or cy5-pda13015-R. Thermal cycling for PCR amplification (5.5 min at 94 °C, followed by 40 cycles of 30 s at 52 °C, and 1.5 min at 72 °C) was carried out to produce single-stranded DNA fragments extracted out of the plasmid genomic DNA. The PCR products were verified their production of single-stranded DNA by 1.5% agarose gel electrophoresis.

3.2. Preparation of human ssDNA targets

An identical process as above was first tried to prepare the human genomic targets, but in vain. A different approach was

Table 2
Oligonucleotide probes and primers used in this study.

Probes	Composition	[a]	Sequences
*a*_1	*ATP5Oc*–*pda06175c*	192 390	5′-amine-C_6-(GTCTTGACAGACATGTCAACATATTTCTCGCCAATGCGCACAATCATTCCACCCAAGATT)-(GTGATTGGACGCGGTGA)3′
*a*_2	*pda06175c*–*ATP5Oc*	390 192	5′-amine-C_6-(GTGATTGGACGCGGTGA)-(GTCTTGACAGACATGTCAACATATTTCTCGCCAATGCGCACAATCATTCCACCCAAGATT)3′
*b*_1	*PSMA5c*–*pda06122c*	203 798	5′-amine-C_6-(GCAGAGCCAATTGCTCGAGCATCACACTGTACAAAGGTCCCAGATGGGTCCATATGAAAC)-(CGGTACCGGAACTCGGA)3′
*b*_2	*pda06122c*–*PSMA5c*	798 203	5′-amine-C_6-(CGGTACCGGAACTCGGA)-(GCAGAGCCAATTGCTCGAGCATCACACTGTACAAAGGTCCCAGATGGGTCCATAT GA AAC)3′
*c*_1	*CANXc*–*pda13015c*	366 129	5′-amine-C_6-(TTAAAGCTCAGCTAGAAGAAAGTGAGGCATGAC ATATACTGTCAACGGAGGGTGAAGGAG)-(ATCGAAGAAC GGCTCGC)3′
*c*_2	*pda13015c*–*CANXc*	129 366	5′-amine-C_6-(ATCGAAGAACGGCTCGC)-(TTAAAGCTC AGC TAGAAGA AAGTGAGGCATGA CATATACTG TCAACGGAGG GTGAAGGAG)3′

Primers	Starting position	Product length ds DNA(bp) ssDNA(b)	Sequences
cy5-pda13015-R	528	528	TGCCTCTCGTCATGGAACAACG
cy5-pda06175-R	690	690	AATTTCATCAGAAACCGAAGGA
cy5-pda06122-R	1020	1020	TTTATTGCGTCAGCATTTCATC
ATP5O-F1	229	524	TTCTGCTGCATCAAAACAGAAT
ATP5O-R1	753		ATGGCAGAAAACCAACACTTTT
cy3-ATP5O-F2	440	313	CGATTAAGCAATACCCAAGGAG
PSMA5-F1	75	709	CTACCCTCGCCATGTTTCTTAC
PSMA5-R1	784		TTCTTCCTTTGTGAACATGTGG
cy3-PSMA5-F2	352	432	TGATAAAGCCAGAGTGGAGACA
CANX-F1	3162	1334	GAGGAGTGACATGAAGCATGAG
CANX-R1	4496		TCTGAGCTGCTGTCCACACTAT
cy3-CANX-F2	3469	1027	GGCTTTCAAATGTACCGATGAT

[a] Complementary section of nucleotide base counted from the 5′ end of the corresponding target.

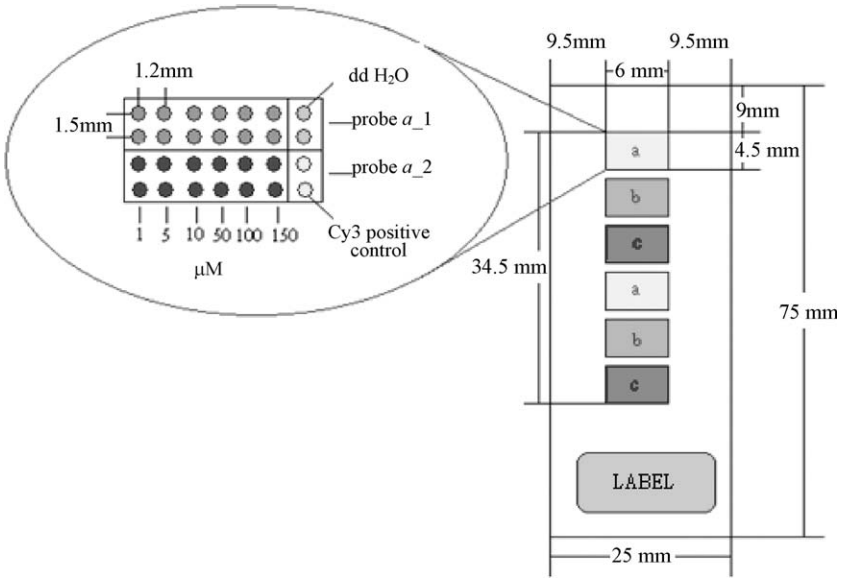

Fig. 2. Microarray layout of objective probes. The probes were spotted in concentrations of, from right to left, 150, 100, 50, 10, 5, and 1 μM. The right-most column is the negative (dd water) and positive control (Sp5-Cy3). Two sets of duplicated 7 × 4-array blocks shown shaded were microarrayed on the chip. Blocks *a*, *b*, and *c* refer to probes *a*, *b*, and *c*. Ten slides were microarrayed in the same batch, which is equal to 9 tests for three sets of probes times three types of DNA targets plus 1 test for the negative target.

therefore conducted. The human *c*DNA was first produced from the total RNA by the reverse-transcript (RT) PCR procedure instructed on the kit. Since low yield of PCR product was obtained upon asymmetrically amplifying the *c*DNA template, we instead processed a regular PCR procedure to generate enough *ds*DNA templates for the subsequent asymmetric PCR. The regular PCR procedure was identical with the asymmetrical one described in the previous section, but with an equal ratio of two none-labeled primers. As indicated in Table 2, they are ATP5O-F1/ATP5O-R1, PSMA5-F1/PSMA5-R1, or CANX-F1/CANX-R1. The consequent PCR products were then separately undergone the asymmetrical PCR with proportion of molar concentration 10–0.2 of the reverse to the second forward primers, cy3-ATP5O-F2, cy3-PSMA5-F2, or cy3-CANX-F2. The production of single-stranded DNA was verified by 1.5% agarose gel electrophoresis.

3.3. Probe microarraying, immobilization, and wash

The probes were spotted in microarrays with a concentration titration of 150, 100, 50, 10, 5, and 1 μM for the objective probes and 25 μM for the control probe. Ten chips were prepared with two duplicated 7 × 4-array blocks (blocks *a*, *b*, and *c*) on each chip as shown in the microarray layout of Fig. 2. The probes were mixed with 20× SSC and 100% glycerol to the final concentrations and loaded onto a 384-hole microtiter plate to perform microarraying, followed by incubation in a humid box at 30 °C for 16–18 h to immobilize the probes on the glass substrates. The spot size was around 600 μm with vertical and horizontal spot-to-spot spacing of 1.5 mm and 1.2 mm. A wash step was then applied to remove the free probes. The DNA chips were first immersed in 2× SSC/SDS for 10-min shaking at 80 rpm. After ddH_2O rinse, the second wash was with 2× SSC in the same condition but without SDS. The final wash was with 0.2× SSC for 10 min, and the slides were rinsed with ddH_2O and spun to dry.

3.4. Hybridization of gene target with the probe

After pre-heating the chips to 50 °C, 45 μl genetic target (made by 10 nM fluorescence-labeled target + 1× hybridization buffer) was spread over the chip surface. The chip surface was covered with a TaKaRa^{TM} spaced cover to form a flat reaction slit chamber. Care was taken to avoid creation of trapped air bubbles. The chip was then enclosed in a humid box and incubated at 50 °C for 2 h. In the post-hybridization treatment, the DNA chips were placed in a container and washed in 2× SSC/SDS for 10 min with shaking at 80 rpm. The chips were then washed with 2× SSC in the same condition but without SDS, followed by another wash with 0.2× SSC for 10 min. Finally, the slides were rinsed with ddH_2O and spun to dry.

3.5. Data acquisition and analysis

The dried chips were scanned by the AXON 4000B scanner with appropriate laser power and PMT settings. The excitation/emission wavelengths of Cy3 were set at 550/570 nm, Cy5 at 649/670 nm, and the scanning resolution at 10 μm. All these parameters were fixed through the study. The raw spot intensities were generated by GenePix Pro version 4.1 software. The analysis process is described as follows. Once the fluorescent images were generated, the software, GenePix Pro 4.1, was executed to analyze the images. It was set to generate a 6 × 4 circle array to cover all microarrayed spots to measure the fluorescent signal. The software then automatically saved the analyzed data as Excel-format files. The calculation of signal average and standard deviation was then manually undertaken over replicate spots. In this study, there were four replicates located in two zones, with two in each zone. The error bars were produced by taking ± half of their standard deviation.

4. Results and discussion

4.1. Negative sample test

To check the non-specific binding of the objective probes, we did a negative sample test by spreading a totally mismatched sample T17-17-Cy3 onto a spotted area and performing hybridization treatments that were identical to the genetic targets to see if any fluorescence was detected. In addition, a specification test as shown in Fig. 3 was also conducted to verify the sequence validation for each probe-target pair. The results showed that the signal detected was less than 0.8% of the lowest reported intensity in Figs. 4–8.

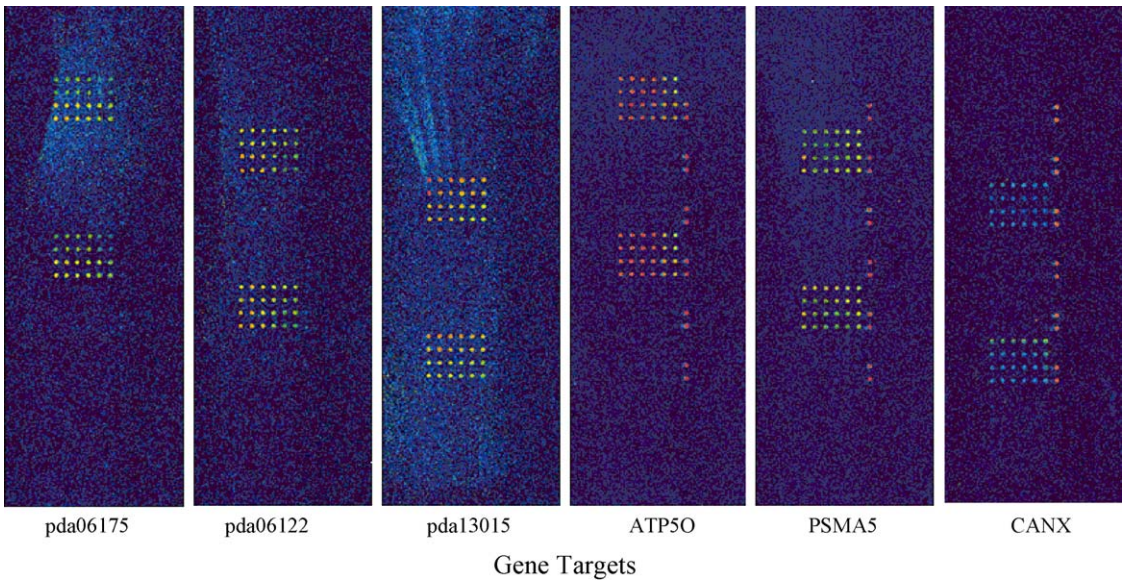

Fig. 3. Sequence validation test for each DNA probe-target pair. Each member of the pair showed perfectly hybridized signals on individual pre-designed microarrayed region. DNA targets pad06175, pda06122, and pda13015 were labeled with cy5 and the other three human genes with cy3 fluorescence dyes.

4.2. Effect of hybridization location on hybridization efficiency

Fig. 4 shows the effect of hybridization location on hybridization efficiency for various DNA target sizes and concentrations. Fig. 4a shows the result for hybridization location close to the slide surface, while Fig. 4b is close to the top free solution phase. Cy3-labeled ATP5O (313b), PSMA5 (432b), and CANX (1027b) served as the model genes individually hybridizing with two sequence-inversed probes. Readers can refer to the corresponding hybridization configurations in Fig. 4c and d, respectively. Comparing Fig. 4a with b indicates that a hybridization location close to the slide surface generally provided better hybridization efficiency than a location close to the free solution, except for ATP5O at high probe concentration. Hybridization at the location close to the free solution above the probe could be easier than that close to the slide surface to allow the shacked wash buffer to wash

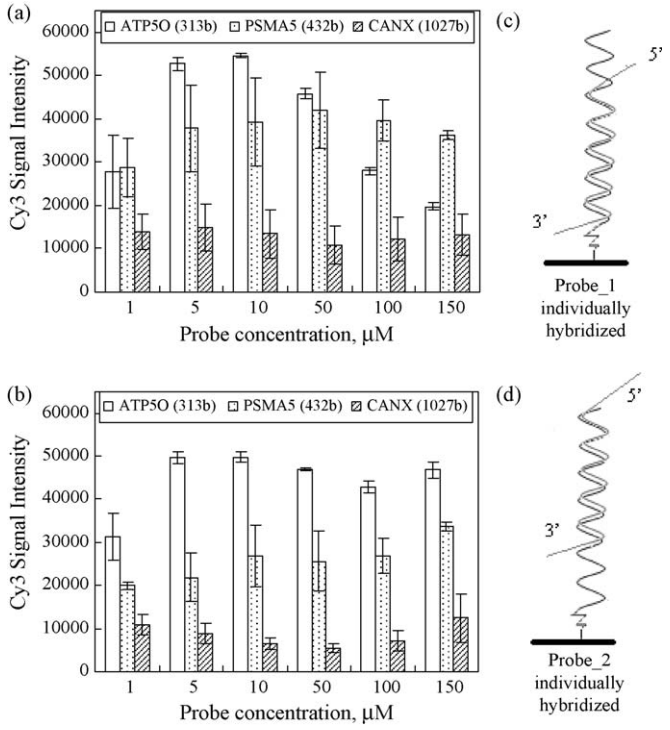

Fig. 4. Effect of hybridization location on hybridization efficiency for various DNA target sizes and concentrations. Cy3-labeled ATP5O (313b), PSMA5 (432b), and CANX (1027b) were individually hybridized with (a) probe_1 (b) probe_2. Their corresponding hybridization configurations are shown in (c) and (d), respectively. The hybridization length is 60mer.

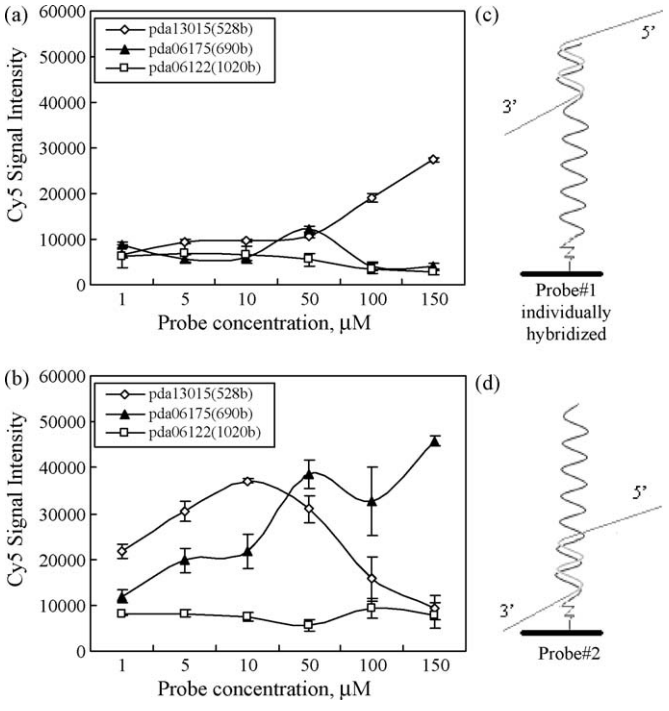

Fig. 5. Effect of hybridization location on hybridization efficiency for a shorter hybridization section for various DNA target sizes and concentrations. Cy5-labeled pda13015 (528b), pda06175 (690b), and pda06122 (1020b) were individually hybridized with (a) probe_1 (b) probe_2. Their corresponding hybridization configurations are shown in (c) and (d), respectively. The hybridization length is 17mer.

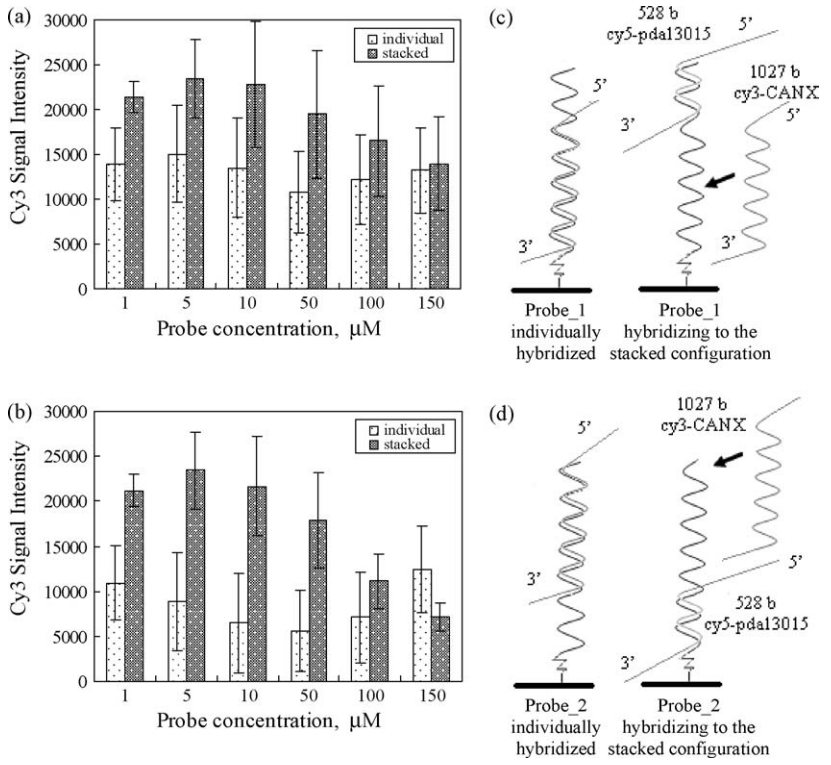

Fig. 6. Signal enhancement by target pre-hybridization. Compared with the individual hybridization, CANX-cy3 (1027b) signal in the stacked configuration was greatly enhanced by the pre-hybridization of pda13015 (528b) on the co-axially shared probes, (a) probe_1, (b) probe_2. Their corresponding hybridization configurations are shown in (c) and (d), respectively.

off the hybridized gene targets. As ATP5O hybridized with probe *a*_1, the signal intensity increased first but then decreased with probe concentration increasing. Although a recent report did not concur that the probe density alone is responsible for the low hybridization efficiency (Mirmomtaz *et al.*, 2008), this parabolic profile is generally explained as the steric hindrance effect caused by a dense probe microarray (Herne and Tarlov, 1997; Peterson *et al.*, 2001) since a dense microarray is believed to reduce the

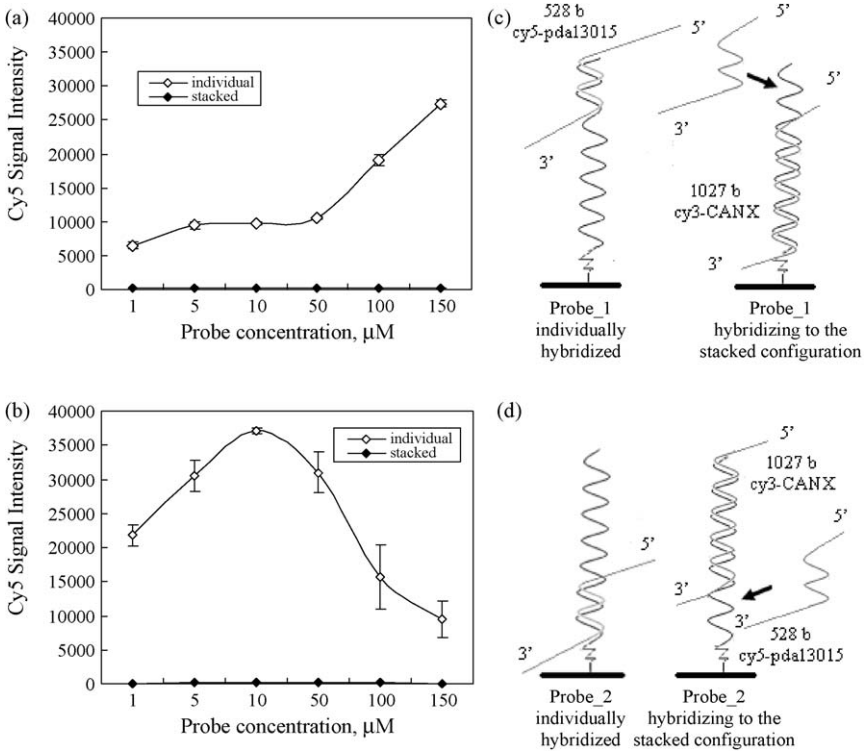

Fig. 7. Signal enhancement by target pre-hybridization. Compared with the individual hybridization, the CANX-cy3 (1027b) signal in the stacked configuration was tremendously enhanced by the pre-hybridization of pda13015 (528b) on their co-axial shared probe, (a) probe_1, (b) probe_2. Their corresponding hybridization configurations are shown in (c) and (d), respectively.

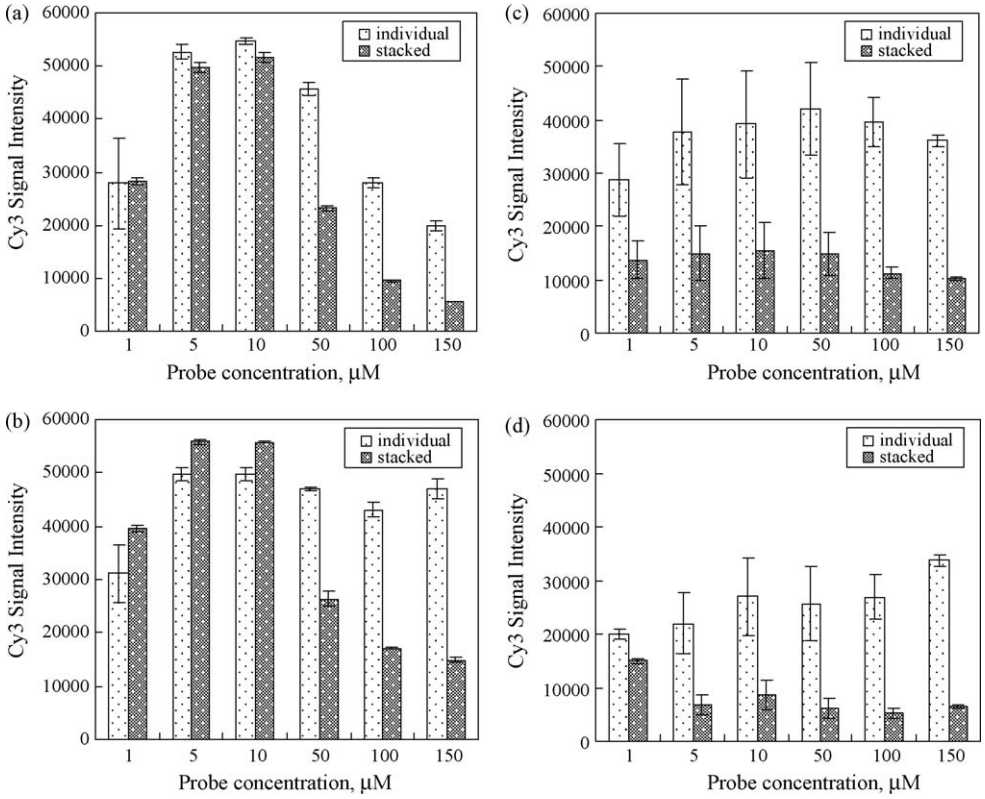

Fig. 8. Effect of relative size of genetic target to its pre-hybridizer on signal enhancement. In addition to the results for CANX(1027b) in Fig. 6, this figure shows the cy3 signal reading for ATO5O(313b) on (a) probe_1, (b) probe_2, and PSMA5(432b) on (c) probe_1, (d) probe_2.

accessibility of free-phase DNA target to the immobilized probe. Its typical profile of measured intensity usually increases first and then drops as the microarrayed probe concentration increases.

Fig. 5 shows a similar test result for a shorter hybridization base–17mer. In this figure, we plotted the signal reading of Cy5 in lines to avoid confusion with the previous bar-graphs of Cy3. With the same implication as Fig. 4, the hybridization location close to the slide surface revealed better hybridization efficiency than one close to the free solution, where target could be more easily de-hybridized from a target-probe hybridized complex by washing. In this scenario, the steric hindrance effect also appeared for pda13015 (528b) on probe_2, but not for other DNA targets.

4.3. Effect of pre-hybridization on hybridization efficiency

Fig. 6 shows the measured Cy3 intensities of gene target CANX (1027b) over various microarrayed concentrations on probe_1 (a) and probe_2 (b). CANX was designed to individually hybridize with the probe or to stack together with the pre-hybridized pda13015 (528b) on the coaxial shared probe. Their corresponding hybridization configurations are shown in Fig. 6c and d. It can be concluded that the stacked configuration clearly received a signal enhancement by the pre-hybridization of pda13015. The enhancement contribution to the overall signal was roughly half fold on probe_1 and 1–3 folds on probe_2. However, this enhancement phenomenon was not observed at high probe concentrations due to the steric effect mentioned above. One possible explanation for this signal enhancement could be that the void space around the probe's bare sections was propped open by the pre-hybridized pda13015, and this void space could facilitate the subsequent CANX docking onto its binding site in the restricted environment. Another reasonable explanation could be the change of probe conformation. The pre-hybridization of pda13015 could cause the tilt probe to stand up, particularly probe_2, where the pre-hybridization occurred in the stem section. The standing conformation of an immobilized probe generally provides better contact with approaching targets than tilted or lying probes (Kaufmann *et al.*, 2008).

4.4. Effect of pre-hybridization order on hybridization efficiency

The next issue of interest was addition inversion of gene targets. Could a similar signal enhancement still be observed from the inverse scenario? In other words, if CANX was added prior to pda13015, could pda13015 receive a similar benefit? Fig. 7 shows the related experimental design and results. The results, however, did not show the expected phenomenon, than moreover, no signal was observed on the stacked configuration. There are two factors that could be responsible: a long-size pre-hybridization of CANX (1027b) and/or a short hybridization section (17mer) of pda13015. In other words, the pre-hybridization of CANX (1027b) could hinder the accessibility of pda13015 (528b) to its complementary probe and/or the section of 17-mer was too short to retain the hybridized complex. The un-hybridized section of CANX hung around the hybridized probe and generated a steric hindrance to pad13015 to access the same probe. The 17-mer short section of pda13015 could be denaturalized by continues washes. In order to clarify the first issue, a further investigation was conducted on the stacking configuration of ATP5O(313b)–pda06175(690b). However, the pre-hybridization of smaller size of ATP5O still caused no signal observed of pda06175 (data not shown). Thus, the signal enhancement by pre-hybridization would not be observed if the gene target designed to receive the benefit was hybridizing in a short section with its probe.

4.5. Effect on hybridization efficiency due to size of pre-hybridizer to relative gene target

Another parameter we examined was the size of pre-hybridization target relative to its up-coming stacking neighbor, and three pairs of gene targets were selected to address this issue. The gene targets to receive the signal enhancement were CANX(1027b), ATP5O(313b), and PSMA5(432b), with 70-mer of hybridization section. Their corresponding pre-hybridizers were pda13015(528b), pda06175(690b), and pda06122(1020b), respectively. For the first pair, CANX was about twice the size of its pre-hybridizer. For the second, ATP5O was shorter, and for the third, PSMA5 was much shorter than its pre-hybridized neighbor. The hybridization configuration for each pair model was carried out identically to Fig. 6c and d. The result for CANX is shown in Fig. 6. Fig. 8 therefore shows the results for the other two gene models.

In Fig. 8a and b, ATP5O performed similar hybridization efficiency in either individual or stacked configurations on two probes for low probe concentration. At high probe concentration, the steric effect was observed on ATP5O such that no signal enhancement was reported. The investigation result for PSMA5 is shown in Fig. 8c and d. In general, PSMA5 did not obtain signal enhancement and was upset by its pre-hybridization partner.

5. Conclusion

The enhancement of hybridization efficiency of a gene target by a DNA pre-hybridizer is reported on two specially designed microarrayed DNA probes and three pair genes of two distinct species. The hybridization efficiency was observed to decrease with increasing probe concentration for a short gene target. This steric effect occurred only when the target was individually hybridized at a location close to the substrate surface. The DNA pre-hybridization greatly enhanced the hybridization efficiency of the subsequent gene target hybridizing onto the coaxial shared probe when a gene target had a large hybridization section and was larger than its pre-hybridization partner. Although a complete experimental design is necessary to obtain more firm conclusions, our results imply that an appropriate design for pre-hybridization of probes can enhance the DNA hybridization efficiency on microarrayed gene chips. This should be useful for optimal experiment design.

Acknowledgments

Financial supports from the National Science Council of Taiwan under Grant No. NSC 98-2221-E-033-022 (JCW) and Chung Yuan Christian University under Grant No. CYCU-98-CR-CE are gratefully acknowledged.

References

Dawson, E., C. Moore, J. Smagala, D. Dankbar, M. Mehlmann, M. Townsend, C. Smith, N. Cox, R. Kuchta, and K. Rowlen, "MChip: A Tool for Influenza Surveillance," *Anal. Chem.*, **78**, 7610 (2006).

Deng, P., Y. Lee, and P. Cheng, "Two-dimensional Micro-bubble Actuator Array to Enhance the Efficiency of Molecular Beacon Based DNA Micro-biosensors," *Biosens. Bioelectron.*, **21**, 1443 (2006).

Fixe, F., H. Branz, N. Louro, V. Chua, D. Prazeres, and J. Condea, "Immobilization and Hybridization by Single Sub-millisecond Electric Field Pulses for Pixel-addressed DNA Microarrays," *Biosens. Bioelectron.*, **19**, 1591 (2004).

Guo, Z., R. Guilfoyle, A. Thiel, R. Wang, and L. Smith, "Direct Fluorescence Analysis of Genetic Polymorphisms by Hybridization with Oligonucleotide Arrays on Glass Supports," *Nucleic Acids Res.*, **22**, 5456 (1994).

Han, Y., H. Liu, H. Zheng, S. Li, and R. Bi, "Purification and Refolding of Human 5-Subunit (PSMA5) of the 20S Proteasome Expressed as Inclusion Bodies in Escherichia coli," *Protein Expres. Purif.*, **35**, 360 (2004).

Herne, T. and M. Tarlov, "Characterization of DNA Probes Immobilized on Gold Surfaces," *J. Am. Chem. Soc.*, **119**, 8916 (1997).

Kan, Y., Y. Wan, F. Beaudoin, D. Leader, K. Edwards, R. Poole, D. Wang, R. Mitchell, and P. Shewry, "Transcriptome Analysis Reveals Differentially Expressed Storage Protein Transcripts in Seeds of Aegilops and Wheat," *J. Cereal Sci.*, **44**, 75 (2006).

Kaufmann, R., I. Averbukh, and R. Naaman, "Controlling the Reactivity of Adsorbed DNA on Template Surfaces," *Langmuir*, **24**, 927 (2008).

Koehler, R. and N. Peyret, "Effects of DNA Secondary Structure on Oligonucleotide Probe Binding Efficiency," *Comput. Biol. Chem.*, **29**, 393 (2005).

Letowski, J., R. Brousseau, and L. Masson, "Designing Better Probes: Effect of Probe Size, Mismatch Position and Number on Hybridization in DNA Oligonucleotide Microarrays," *J. Microbiol. Meth.*, **57**, 269 (2004).

Liu, Z., X. Zhang, N. He, Z. Lu, and Z. Chen, "Probing DNA Hybridization Efficiency and Single Base Mismatch by X-ray Photoelectron Spectroscopy," *Colloid Surf. B-Biointerfaces*, **71**, 238 (2009).

Lorkovic, Z., "Role of Plant RNA-binding Proteins in Development, Stress Response and Genome Organization," *Trends Plant Sci.*, **14**, 229 (2009).

Mao, X., Y. Ma, A. Zhang, L. Zhang, L. Zeng, and G. Liu, "Disposable Nucleic Acid Biosensors Based on Gold Nanoparticle Probes and Lateral Flow Strip," *Anal. Chem.*, **81**, 1160 (2009).

Maruyama, A., M. Ueda, W. Kim, and T. Akaike, "Design of Polymer Materials Enhancing Nucleotide Hybridization for Anti-gene Technology," *Adv. Drug Deliv. Rev.*, **52**, 227 (2001).

McQuain, M., K. Seale, J. Peek, T. Fisher, S. Levy, M. Stremler, and F. Haseltona, "Chaotic Mixer Improves Microarray Hybridization," *Anal. Biochem.*, **325**, 215 (2004).

Mirmomtaz, E., M. Castronovo, C. Grunwald, F. Bano, D. Scaini, A. Ensafi, G. Scoles, and L. Casalis, "Quantitative Study of the Effect of Coverage on the Hybridization Efficiency of Surface-bound DNA Nanostructures," *Nano Lett.*, **8**, 4134 (2008).

Mootha, V., C. Lindgren, K. Eriksson, A. Subramanian, and S. Sihag, "PGC-1alpha-responsive Genes Involved in Oxidative Phosphorylation are Coordinately down Regulated in Human Diabetes," *Nat. Genet.*, **34**, 267 (2003).

Peterson, A., R. Heaton, and R. Georgiadis, "The Effect of Surface Probe Density on DNA Hybridization," *Nucleic Acids Res.*, **29**, 5163 (2001).

Peytavi, R., L. Tang, F. Raymond, K. Boissinot, L. Bissonnette, M. Boissinot, F. Picard, A. Huletsky, M. Ouellette, and M. Bergeron, "Correlation between Microarray DNA Hybridization Efficiency and the Position of Short Capture Probe on the Target Nucleic Acid," *BioTechniques*, **39**, 89 (2005).

Razumovitch, J., K. deFranca, F. Kehl, M. Wiki, W. Meier, and C. Vebert, "Optimal Hybridization Efficiency upon Immobilization of Oligonucleotide Double Helices," *J. Phys. Chem. B*, **113**, 383 (2009).

Rule, G., R. Montagna, and R. Durst, "Characteristics of DNA-tagged Liposomes Allowing Their Use in Capillary-migration Sandwich-hybridization Assays," *Anal. Biochem.*, **244**, 260 (1997).

Ruuska, S., T. Girke, C. Benning, and J. Ohlrogge, "Contrapuntal Networks of Gene Expression during Arabidopsis Seed Filling," *Plant Cell*, **14**, 1191 (2002).

Sandoval, F., Y. Zhang, and S. Roje, "Flavin Nucleotide Metabolism in Plants: Monofunctional Enzymes Synthesize FAD in Plastids," *J. Biol. Chem.*, **283**, 30890 (2008).

Sreekumar, R., P. Halvatsiotis, J. Schimke, and K. Nair, "Gene Expression Profile in Skeletal Muscle of Type II Diabetes and the Effect of Insulin Treatment," *Diabetes*, **51**, 1913 (2002).

Takizawa, T., K. Tatematsu, K. Watanabe, K. Kato, and Y. Nakanishi, "Cleavage of Calnexin Caused by Apoptotic Stimuli: Implication for the Regulation of Apotosis," *J. Biochem.*, **136**, 399 (2004).

Tao, S., H. Gao, F. Cao, X. Ma, and J. Cheng, "Blocking Oligo-A Novel Approach for Improving Chip-based DNA Hybridization Efficiency," *Mol. Cell. Probes*, **17**, 197 (2003).

Wang, S. and Q. Cheng, "Microarray Analysis in Drug Discovery and Clinical Applications," *Method Mol. Biol.*, **316**, 49 (2005).

Wu, P., P. Hogrebe, and D. Grainger, "DNA and Protein Microarray Printing on Silicon Nitride Waveguide Surfaces," *Biosens. Bioelectron.*, **21**, 1252 (2006).

Yang, D., J. Huang, C. Chen, H. Su, and J. Wu, "Enhancement of Target-DNA Hybridization Efficiency by Pre-hybridization on Sequence-Orientated Micro-arrayed Probes," *J. Chin. Inst. Chem. Engrs.*, **39**, 187 (2008).

Zammatteo, N., L. Jeanmart, S. Hamels, S. Courtois, Louette, L. Hevesi, and J. Remacle, "Comparison between Different Strategies of Covalent Attachment of DNA to Glass Surfaces to Build DNA Microarrays," *Anal. Biochem.*, **280**, 143 (2000).